Magnetic enhancement in antiferromagnetic nanoparticle of $CoRh_2O_4$

R. N. Bhowmik,[1,*] R. Nagarajan,[2] and R. Ranganathan[1]
[1]*Experimental Condensed Matter Physics Division, Saha Institute of Nuclear Physics, 1/AF, Bidhannagar, Calcutta 700064, India*
[2]*Tata Institute of Fundamental Research, Solid State Condensed Matter Physics Division, Mumbai, India*
(Received 19 August 2003; published 27 February 2004)

Our magnetic investigation of $CoRh_2O_4$ nanoparticles show the signature of antiferromagnetic ordering at $T_N \approx 27$ K, same as that of the bulk sample, for all particle sizes down to ≈ 16 nm. However, we observe a systematic magnetic enhancement below T_N, being larger for a smaller particle size. We propose a core-shell model for the magnetization of nanoparticles, with the core retaining its antiferromagnetic order and the enhancement of magnetization below T_N attributed to the increasing number of frustrated shell (surface) spins. The scaling analysis of low temperature magnetization shows that the system approaches the limit of superparamagnetism for the particle size ~ 8 nm. Our model also predicts an alternation of exchange interactions along the inter-particle distance, very similar to RKKY type interactions in the metallic spin glass systems.

DOI: 10.1103/PhysRevB.69.054430 PACS number(s): 75.40.Cx, 75.30.Kz, 75.50.Lk

I. INTRODUCTION

Neel[1] predicted the existence of superparamagnetism and weak ferromagnetism in an antiferromagnetic nanoparticle (AFN). It has also been predicted that a change of the degeneracy and topology of the antiferromagnetic ground state of a geometrically frustrated system, due to the introduction of nonmagnetic dilution,[2] due to a reduction of the particle size,[3] or due to strain induced disorder[4] may lead to a quantum spin fluctuation effect with a superparamagnetic behavior persisting down to 0 K. These facts provide recent interest for the investigation of the AFN.[3]

The spinel oxides with formula unit AB_2O_4 (Ref. 5) represent one of the most important and interesting families of magnetic materials, where the competition between various type of superexchange interactions (J_{AB}, J_{BB}, and J_{AA}) and finite size effects of the nanoparticle exhibit superparamagnetism,[6] surface spin canting,[7] and site disorder[8] effects. Most of the reports[6–9] of those nanoparticle spinels where magnetic moments are occupied either at the site *B* or at both *A* and *B* sites. The search for nanoparticle of antiferromagnetic spinel having magnetic moment only at A sites are also interesting because of their geometrical frustration effect.[9,10] Recently, Sato *et al.*[10] have shown a variety of magnetic states in the nanoparticles of antiferromagnetic Co_3O_4, where the *B* sites are occupied by nonmagnetic Co^{3+} and *A* sites are occupied only by magnetic Co^{2+} moments. These considerations motivated us to investigate the magnetic properties of mechanical milled $CoRh_2O_4$. $CoRh_2O_4$ is derived from Co_3O_4, where Co^{3+} is replaced by nonmagnetic Rh^{3+} ($4d^6$) ions and the structure $(Co^{2+})_A[Rh_2^{3+}]_BO_4$ for a bulk $CoRh_2O_4$ spinel has magnetic moment Co^{2+} occupying at the *A* sites alone and the long range antiferromagnetic order below $T_N = 27$ K is due to Co^{2+}-O^{2-}-Co^{2+} (J_{AA}) superexchange interactions alone.

II. EXPERIMENTAL RESULTS AND DISCUSSION

Bulk $CoRh_2O_4$, prepared by the standard solid state sintering method, was mechanical milled in a 80-ml agate vial with 10-mm agate balls with a ball to sample mass ratio of 12:1 using Fritsch Planetary Mono Mill ''Pulverisette 6.'' The milled samples are designated as mhX, where X denotes the number of milling hours. The x-ray diffraction spectra (XRD) of milled samples, using Philips PW1710 diffractometer with Cu K_α radiation, are matched to the spinel structure of the bulk sample without any additional phase. The systematic broadening of XRD lines with milling time corresponds to the decrease of particle size and is confirmed from *both of transmission electron micrographs (TEM) data (Table 1) and analyzing XRD 311 line broadening using Debye-Scherrer equation (the results are not shown in Table I). However, we do not find the effect of recombination of particles up to our 60-h milling to produce a 16-nm particle, as observed in some mechanical alloyed spinels where the particle size has shown increasing trend after a critical milling hour.*[11,12] Since the particles size encounted are below 100 nm, the nanoparticles in the present study are essentially single grained particles. From Table I, we see that the lattice parameter, determined by considering all XRD peaks, of the nanoparticle samples, even though showing very small decreasing trend with the particle size, are not significantly changed with respect to bulk sample. *We have found that the XRD peaks of milled samples, as shown for the 311 line in Fig. 1, show a small shift to a higher scattering angle* (2θ) *with respect to the bulk sample. In the case of a nanoparticle spinel oxide, for example, in mechanical milled*

TABLE I. Particle size *D* from TEM photographs, lattice parameter $a(\pm 0.002$ Å) from XRD data, 311 peak position (2θ) from the XRD data, effective paramagnetic moment (μ_{eff}) from the *M* vs *T* data, paramagnetic Curie temperature (θ_p) from *M* vs *T* data, and milling time (T_{mill} in hours).

Sample	T_{mill}	D (nm)	a (Å)	2θ (deg)	$\mu_{eff}(\mu_B)$	θ_p (K)
bulk	0h	few μm	8.466	35.47	4.60	−44.2
mh12	12h	70±1	8.482	35.56	4.60	−42.8
mh24	24h	50±1	8.457	35.75	4.61	−42.0
mh36	36h	32±1	8.449	35.71	4.63	−41.8
mh48	48h	19±1	8.468	35.67	4.65	−43.8
mh60	60h	16±1	8.459	35.64	4.76	−51.0

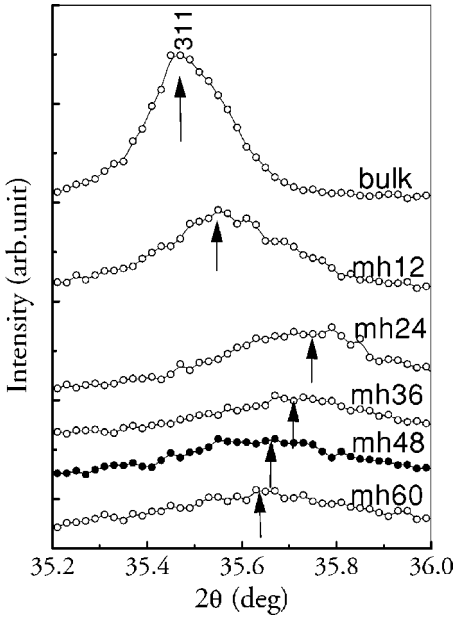

FIG. 1. 311 peak of XRD spectra of bulk and milled samples. The arrow indicates the position of the 311 peak.

$ZnFe_2O_4$,[13]*the change of lattice parameter with particle size has been reflected in the alternation of antiferromagnetic ordering temperature* (T_N) *and attributed to the site exchange of cations. Our magnetic measurements, described below, show that there is no change of* $T_N(\approx 27\ K)$ *with decreasing particle size. Therefore, we suggest that the shift of peak position is due to a small mechanical strain induced effect which includes the effect of some surface disorder*, but certainly not due to chemical disorder, *i.e.*, site exchange of atoms in lattices as observed in mechanical milled $ZnFe_2O_4$.[8]

The dc magnetization under zero field cooled (ZFC) and field cooled (FC) condition of the samples, using a superconducting quantum interference device (Quantum Design, USA) magnetometer, are shown in Fig. 2. The inset of Fig. 2 (left scale) shows the antiferromagnetic ordering temperature at $T_N \approx 27.5\ \mathrm{K} \pm 0.5\ \mathrm{K}$ for bulk sample. The magnetization data at $T > 50$ K fits well to Curie-Weiss law (inset, right scale)

$$H/M = \frac{C}{T - \theta_p}. \tag{1}$$

The Curie constant ($C = \mathrm{N}\mu_{eff}^2/3k$, N is the number of $CoRh_2O_4$ formula unit per gram of the sample) gives the effective paramagnetic moment $(\mu_{eff}) = (4.60 \pm 0.10)\mu_B$ per formula unit for the bulk sample, which is consistent with the reported value $\mu_{eff} = 4.55\mu_B$.[14] The paramagnetic Curie temperature $(\theta_p) \approx -(45 \pm 2)$ K is consistent with antiferromagnetic order.

We now discuss some of the interesting magnetic aspects of the nanoparticle samples. The antiferromagnetic order is retained around the same temperature (at $T_N \approx 27.5$ K) even for the sample with a particle size ~ 16 nm (see Fig. 2). Further, it is observed that the FC magnetization is higher

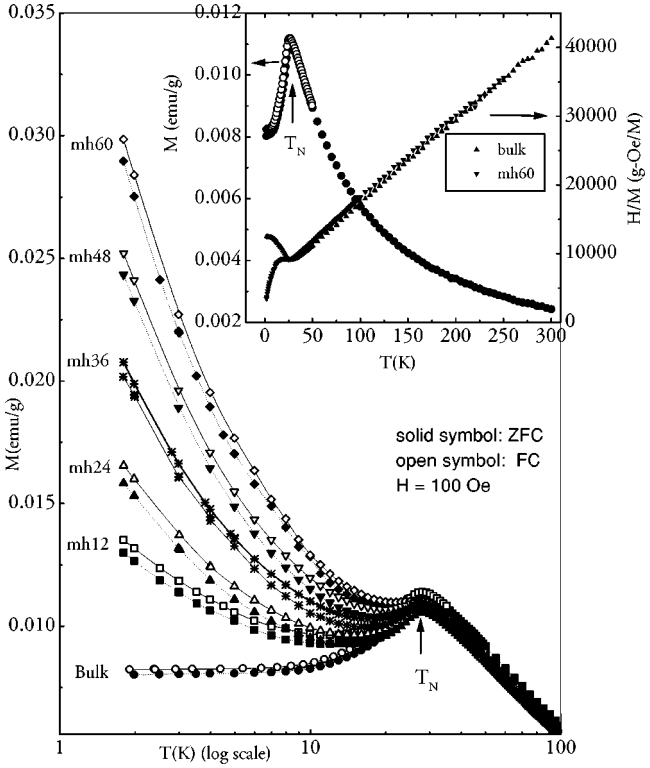

FIG. 2. dc magnetization at $H = 100$ Oe for bulk (inset, left scale) and milled samples with bulk sample (main panel, semilog scale). Lines are to guide to the eye. The linearity of the time H/M vs T plot (inset) above 50 K for bulk and mh60 samples suggest the Curie-Weiss nature of magnetization data.

than the ZFC magnetization below T_N, which suggests a field induced metastable magnetic state during the field cooling process of the samples.[9] The magnetization data of milled samples also follow the Curie-Weiss law at $T > 50$ K. As an example, the inset of Fig. 2 (right scale) shows linearity in H/M vs T data for the mh60 sample above 50 K. The fit results of Eq. (1) for all samples are shown in Table I. The negative value of θ_p for all the mhX samples indicates that an antiferromagnetic exchange interaction is dominant in the nanoparticles. Interestingly, the effective paramagnetic moment (μ_{eff}) shows a systematic increase with a decreasing particle size, *viz*, $4.60\mu_B$/formula unit for the bulk sample increases to about $4.76\mu_B$/formula unit for the sample of particle size 16 nm. This significant increase of μ_{eff} with decreasing particle size in our samples may have several possibilities, e.g., (1) the existence of isolated Co nanoparticles with reduced coordination number in surface spins,[15] (2) site exchange of cations,[8,9] and (3) an electron spin polarization effect in the $3d(\mathrm{Co}) - 4f(\mathrm{Rh})$ system.[16] Since we have not used Co metals for the sample preparation and mechanical milling was carried out in atmospheric condition, we did not expect an isolated Co nanoparticle. The recent results of Peng *et al.*[17] suggest that the spin bilayer, consisting of a ferromagnetic Co core and an antiferromagnetic CoO shell, has superparamagnetic blocking about 200 K which is much higher than our $T_N \approx 27$ K. So the change in μ_{eff} is not due to Co nanoparticles. Since $T_N \approx 27$ K remains unchanged, the enhancement in μ_{eff} in our nanopar-

ticle samples are not due to the site exchange of cations (Co^{2+} and Rh^{3+}) which has shown its association with the alternation of T_N in other nanoparticle spinels.[8,9] Therefore, the enhancement of μ_{eff} in our nanoparticle samples is most probably due to the electronic spin polarization effect or spin-orbital coupling, as found in the $3d$(Co)-$4d$(Rh) system.[16] The other uniqueness in Fig. 2 is that all of the nanoparticles show, *below* T_N, an *increase* in magnetization with *decreasing* temperature. This increase in the low temperature magnetization systematically depends on the particle size, being larger for smaller particle size. This low temperature increase of magnetization gives the character which is similar to a spin bilayer system like $Ni_{81}Fe_{19}/CoO$,[18] where the sharp increase of low temperature magnetization has been attributed to the number of uncompensated (frustrated) interfacial spins. The increase of the low temperature magnetization is also not consistent with the core-shell model, proposed by Kodama *et al.*[7] for a $NiFe_2O_4$ nanoparticle system. In this model core remains ferrimagnetic and the shell (thin surface layer) forms a canted spin structure. The surface spin canting increases with decreasing particle size and, hence, decreases over all magnetization of the $NiFe_2O_4$ nanoparticle. In our case, we have seen an increase in the magnetization as the particle size decreases. This is because of different kind of nanoparticle systems. Kodama *et al.*[7] started with a long range order ferrimagnetic spinel $NiFe_2O_4$, where both *A* and *B* sites are occupied by magnetic Fe^{3+} moments. In our case, as we discussed that $CoRh_2O_4$ is an antiferromagnetic spinel where magnetic Co^{2+} moments occupy only *A* sites. In system, as we have, the antiparallel spins arrangement gives the lowest magnetic contribution. If the surface spin canting increases, an increase (*not the decrease*) of surface magnetism is expected. Chen *et al.*[19] explained the enhancement of the magnetization in Co nanoparticles in terms of core-shell picture, but all core-shell pictures to our knowledge are based on ferromagnet or ferrimagnetic nanoparticles. The above discussion and our experimental data clearly indicate the limitation of core-shell model, proposed by Kodama *et al.*[7] for an antiferromagnetic nanoparticle.

Therefore, we propose a core-shell model for AFNs where the core is essentially antiferromagnetic and the shell consists of frustrated spins. We also discuss below the combined aspect of the core-shell model of Kodama *et al.*[7] and the spin bilayer concept of Takano *et al.*[18] in our proposed core-shell model. The Heisenberg exchange interactions between two neighboring spins are expressed as

$$H_{EX} \propto J_{EX} \Sigma_{ij} S_i S_j \cos\theta_{ij}, \tag{2}$$

where θ_{ij} is the angle between spins i and j and $0° \leqslant |\theta_{ij}| \leqslant 180°$. Total magnetization of the particle will be

$$M = \alpha M_{shell} \Sigma_{ij} \cos\theta_{ij} + (1-\alpha) M_{core}, \tag{3}$$

where α is the shell thickness, which increases with decreasing particle size. From the above two equations, we attribute θ_{ij} as the important factor which controls the exchange interactions and magnetization of nanoparticles. For core spins, θ_{ij} is 180° and any value of $\theta_{ij} < 180°$ shell spins also takes

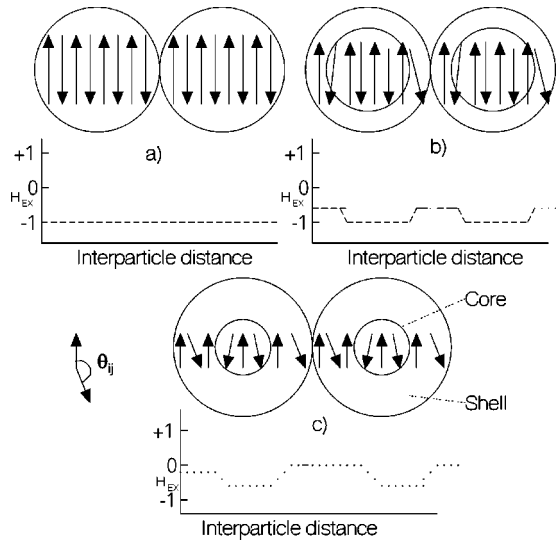

FIG. 3. A schematic diagram (two dimensional); arrows represent the spins. (a) Perfect antiferromagnetic order (AFM) of spins in a bulk sample gives $H_{EX} = -1$. (b) For nanoparticles, the core (inside small circles) spins are almost antiparallel with slight distortion near the shell (in between two core) and the deviation of shell spins from the AFM arrangement make the H_{EX} value to less negative in the shell regions. θ_{ij} is the angle between two adjacent shell spins. (c) For a very small particle size, the shell deviates more from the AFM arrangement and even the core spins also show a less AFM configuration. Consequently, H_{EX} becomes more modulated and less negative and shows alternation of more negative and less negative.

into account the effect of the multisublattice spin configuration of the surface, as suggested to explain the magnetic enhancement in the AFN of NiO.[3] The schematic diagram [Fig. 3(a)] shows that the long range antiferromagnetic interactions for the bulk sample spans up to many particles without any modulation. *However, we are describing our model for a nanoparticle system where a large number of nanos exist side by side to have interparticle interactions. Some of the particles may be in close contact and some of them may be slightly away from each other. In the limiting case, when two nanoparticles are in contact* [*Fig. 3(b)*], the antiferromagnetic core is surrounded by a shell of frustrated spins and the antiferromagnetic interactions between two adjacent cores are modulated by shell spins. When α increases, more and more numbers of shell spins break their antiferromagnetic (180°) configuration. Consequently, there is an alternation (modulation) of antiferromagnetic and less antiferromagnetic regions. Finally, after a critical value of α and hence a critical value of the particle size, θ_{ij} will show the values of random distribution. This brings the net exchange fields (H_{EX}) near to zero value [Fig. 3(c)]. The alternation of antiferromagnetic and less antiferromagnetic regions over many particles is very similar to the RKKY picture of metallic spin glasses.[20] This situation, where spins of the particle are highly frustrated, is consistent with Neel's prediction of superparamagnetism in an antiferromagnetic nanoparticle.[1] Our picture may be further consistent with Neel's prediction of weak ferromagnetism,[1] if the J_{EX} value

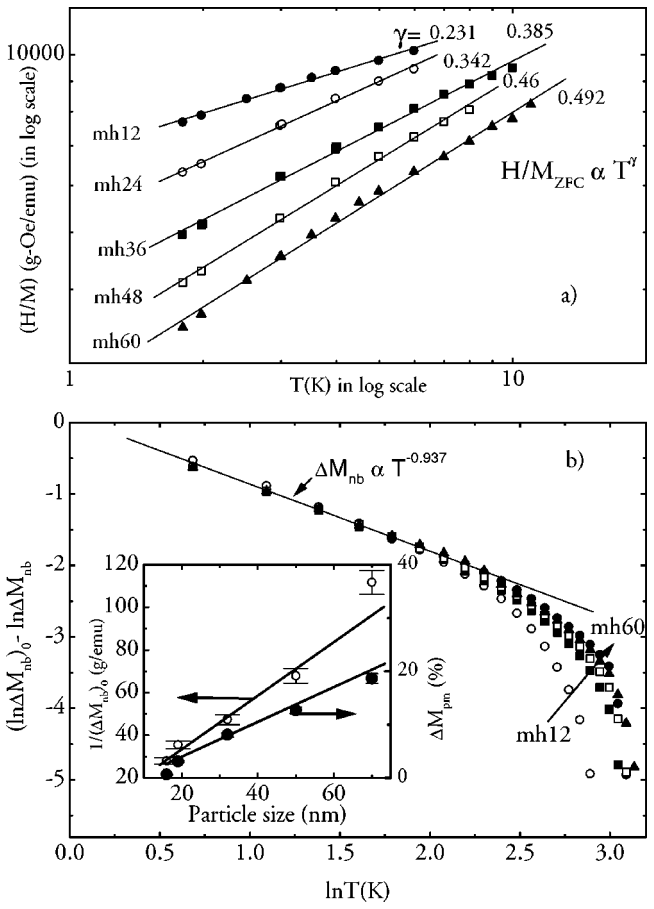

FIG. 4. Log-log plot shows the fit of $H/M \propto T^{\gamma}$ below 10 K for nanoparticle samples. (b) Magnetization of nanoparticles over a bulk sample (ΔM_{nb}) follows a scaling function up to 10 K and deviates at higher temperature. The inset of (b) shows that $(\Delta_{nb})_0$ is inversely and ΔM_{pm} linearly proportional to the particle size. Experimental data and fit data are represented by point symbols and lines, respectively.

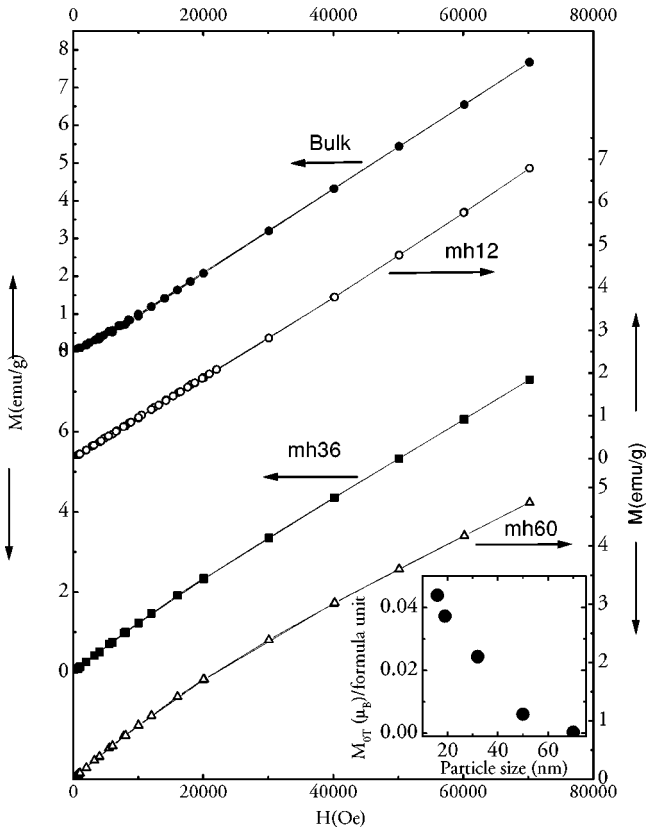

FIG. 5. M vs H for bulk and nanoparticle $CoRh_2O_4$ samples. Left and right arrows indicate the M axis for the corresponding sample. The inset shows the linear extrapolated value of $M_{0T}(\mu_B)$ for different particles.

crosses the zero value and this, we believe, can occur as a (high) magnetic field induced effect. We now use our proposed core-shell model to explain the ZFC magnetization data below. The increase of magnetization at $T \ll T_N$ is very similar to a para/superparamagnetic or ferrimagnetic contribution[9,10] of frustrated spins.[18] The H/M_{ZFC} vs T data of milled samples show a downward curvature below 10 K, whereas the log-log plot [Fig. 4(a)] shows that $H/M_{ZFC} \propto T^{\gamma}$ below 10 K. The constant value γ systematically increases from 0.23 (for the mh12 sample) to 0.49 (for the mh60 sample). The exponent (γ) for the mh60 sample is, still, far below the typical paramagnetic/superparamagnetic value 1. We attribute this deviation to the coexistence of frustrated shell spins and antiferromagnetic core spins. The increase of the γ value with decreasing particle size indicates that the shell contribution is increasing with decreasing particle size. For the subtraction of the antiferromagnetic background of the core, we have subtracted the ZFC magnetization of the bulk sample from the ZFC magnetization of nanoparticle samples, and this is quantified as ΔM_{nb} ($=M_{zfc}^{nano}-M_{zfc}^{bulk}$). In order to test the closeness of γ to 1, we first estimate the value of ΔM_{nb} at the $T=0$ limit, i.e., $(\Delta M_{nb})_0$, by a linear extrapolation of $\ln[\Delta M_{nb}]$ vs $\ln[T]$ plot for all the nanoparticle samples. We find that the magnetization data below 10 K obey the following scaling law [Fig. 4(b)]:

$$\Delta M_{nb} = (\Delta M_{nb})_0 T^{-(0.937 \pm 0.002)}. \tag{4}$$

The exponent (≈ 0.937) is still below 1, and indicates that the antiferromagnetic order of core still affects the superparamagnetic behavior of the shell. The deviation of the higher temperature data from the scaling is due to the dominant antiferromagnetic contribution of cores. The inverse variation of $(\Delta M_{nb})_0$ with particle size [inset of Fig. 4(b)] corresponds to the increase of the frustrated shell spin density.[18] The magnetization around 15 K (Fig. 2) also reveals the competition between shell and core spins, where the antiferromagnetic order of core increases the magnetization above 15 K up to T_N and the superparamagnetic type contribution of shell increases magnetization below 15 K. Consequently, the difference between the peak magnetization M_{ZFC}^{peak} at T_N and the minimum of magnetization M_{ZFC}^{min} below T_N estimates the magnetic contribution of the shell. Indeed, the decrease of $\Delta M_{pm}=(M_{ZFC}^{peak}-M_{ZFC}^{min})\times 100/M_{ZFC}^{peak}$ from 18% (for the mh12 sample) to 0.6% (for the mh60 sample) confirms that, below T_N, the antiferromagnetic contribution from the core is decreasing with particle size. The linear

variation of ΔM_{pm} vs particle size [Fig. 4(b) inset] suggests that there will be no magnetization minimum below T_N or rather no T_N for the particle size ≈ 8 nm, and this may be the critical size for this system below which the nanoparticle will exhibit typical a superparamagnetic behavior.

The magnetization (M) data at 5 K with magnetic field (H) up to 7 T (Fig. 5) confirms the long range antiferromagnetic order of the bulk sample, and the mh12 sample does not show a significant change with respect to the bulk. However, the down curvature in the M vs H data of mh36 and mh60 samples at higher magnetic fields suggests the increase of an additional magnetic order as the particle size decreases. The Arrot plot (M^2 vs H/M) analysis does not give any spontaneous magnetization for any samples, which further confirms that the additional magnetic contribution is not due to long range ferromagnetic/ferrimagnetic type. Rather, the nonlinear increase of the magnetization without a hysteresis loop establishes that the superparamagnetic behavior becomes more dominant for the smaller nanoparticles. The linear extrapolation of the high field ($H \geqslant 4$ T) magnetization to $H=0$ gives the measure of the induced magnetic moment M_{0T}. The increase of M_{0T} values (Fig. 5, inset) with decreasing particle size is consistent with the predicted induced magnetic moment or weak ferromagnetism in the frustrated antiferromagnetic nanoparticles.[1,21] This is also consistent with our prediction that field induced magnetic order may appear for the smaller antiferromagnetic nanoparticle.

III. CONCLUSIONS

In conclusion, a magnetic enhancement in mechanical milled nanoparticles of antiferromagnetic spinel $CoRh_2O_4$ is reported. *The antiferromagnetic ordering temperature* T_N (~ 27 K), *as seen for the bulk sample, is retained down to our lowest particle size of 16 nm. This result is of fundamental difference compared to the other nanoparticle spinels, and confirms that there is no site exchange of cations* (Co^{2+} *and* Rh^{3+}) *in our nanoparticle spinel*. A small but systematic increase in the effective paramagnetic moment (μ_{eff}) with decreasing particle size is attributed to the spin-orbital coupling effect. However, we interpret the considerable enhancement of magnetization below T_N in terms of a core-shell model. From a theoretical point of view, $CoRh_2O_4$ nanoparticles may be considered as an ideal material for studying the spin frustration effect geometrically in an antiferromagnetic system with a magnetic ion (Co) confined only to an A site alone. The most important point is that the surface magnetism with particle size is free from the complexity of the site exchange of cations in this system, which may find its applications in multilayers.

ACKNOWLEDGMENT

One of the authors (R.N.B.) thanks Council of Scientific and Industrial Research (CSIR, India) for providing fellowship [F.No.9/489(30)/98-EMR-I].

*Email address: rnb@cmp.saha.ernet.in, Present address: Mahishadal Raj college, Mahishadal, East Midnapur, West Bengal, Pin Code 721628, India.

[1] L. Neel, in *Low Temperature Physics*, edited by C. Dewitt, B. Drefus, and P.D. de Gennes (Gordon and Beach, New York, 1962), p. 413.
[2] C.L. Henley, Phys. Rev. Lett. **62**, 2056 (1989).
[3] R.H. Kodama, S.A. Makhlouf, and A.E. Berkowitz, Phys. Rev. Lett. **79**, 1393 (1997).
[4] H. Reichert, V.N. Bugaev, O. Shchyglo, A. Schöps, Y. Sikula, and H. Dosch, Phys. Rev. Lett. **87**, 236105 (2001).
[5] S. Krupika and P. Novak, in *Ferromagnetic Materials*, edited by E.P. Wolfarth (North-Holland, Amsterdam, 1982), Vol. 3, p. 189.
[6] *Magnetic Properties of Fine Particles*, edited by J.L. Dorman and D. Fiorani (North-Holland, Amsterdam, 1991).
[7] R.H. Kodama, A.E. Berkowitz, E.J. McNiff, Jr., and S. Foner, Phys. Rev. Lett. **77**, 394 (1996).
[8] H.H. Hamdeh, J.C. Ho, S.A. Oliver, R.J. Willey, G. Oliveri, and G. Busca, J. Appl. Phys. **81**, 1851 (1997).
[9] X.H. Chen, H.T. Zhang, C.H. Wang, X.G. Luo, and P.H. Li, Appl. Phys. Lett. **81**, 4419 (2002).
[10] M. Sato, S. Kohiki, Y. Hayakawa, Y. Sonda, T. Babasaki, H. Deguchi, and M. Mitome, J. Appl. Phys. **88**, 2771 (2000).
[11] R.N. Bhowmik and R. Ranganathan, J. Mater. Sci. **37**, 4391 (2002).
[12] V.G. Harris, D.J. Fatemi, J.O. Cross, E.E. Carpenter, V.M. Browning, J.P. Kirkland, A. Mohan, and G.J. Long, J. Appl. Phys. **94**, 496 (2003).
[13] C.N. Chinnasamy, A. Narayanasamy, N. Ponpandian, K. Chattopadhyay, H. Guerault, and J.-M. Greneche, J. Phys.: Condens. Matter **12**, 7795 (2000).
[14] G. Blasse and D.J. Schipper, Phys. Lett. **5**, 300 (1963).
[15] F. Liu, M.R. Press, S.K. Khanna, and P. Jena, Phys. Rev. B **39**, 6914 (1989).
[16] D. Zitoun, M. Respaud, M. Fromen, M.J. Casanove, P. Lecante, C. Amiens, and B. Chaudret, Phys. Rev. Lett. **89**, 037203 (2002).
[17] D. Peng, K. Sumiyama, T. Hihara, S. Yamamuro, and T. Konno, Phys. Rev. B **61**, 3103 (2000).
[18] K. Takano, R.H. Kodama, A.E. Berkowitz, W. Cao, and G. Thomas, Phys. Rev. Lett. **79**, 1130 (1997).
[19] J.P. Chen, C.M. Sorensen, K.J. Klabunde, and G.C. Hadjipanayis, Phys. Rev. B **51**, 11527 (1995).
[20] J.A. Mydosh, *Spin Glasses, An Experimental Introduction* (Taylor & Francis, London, 1993).
[21] M.E. Zhitomirsky, A. Honecker, and O.A. Petrenko, Phys. Rev. Lett. **85**, 3269 (2000).